Contents lists available at ScienceDirect

Robotics and Autonomous Systems

EMG-based decoding of grasp gestures in reaching-to-grasping motions

I. Batzianoulis [a],[*], S. El-Khoury [a], E. Pirondini [b], M. Coscia [b], S. Micera [b],[c], A. Billard [a]

[a] *Learning Algorithms and Systems Laboratory (LASA), School of Engineering, École Polytechnique Fédérale de Lausanne (EPFL), Lausanne, Switzerland*
[b] *Bertarelli Foundation Chair in Translational Neuroengineering, Center for Neuroprosthetics and Institute of Bioengineering, School of Engineering, École Polytechnique Fédérale de Lausanne (EPFL), Lausanne, Switzerland*
[c] *The Biorobotics Institute, Scuola Superiore SantAnna, Pisa, Italy*

HIGHLIGHTS

- Decode of the grasp type by Electromyography on the early stages of the reach-to-grasp motion.
- Possible to decode the grasp type during the preshaping of the hand.
- Possible generalization over different positions of the object near the training position.
- A robotic implementation showed that it possible to express accurately the intention of the grasp type through a robotic hand during the reaching motion and before grasping the object.

ARTICLE INFO

ABSTRACT

Predicting the grasping function during reach-to-grasp motions is essential for controlling a prosthetic hand or a robotic assistive device. An early accurate prediction increases the usability and the comfort of a prosthetic device. This work proposes an electromyographic-based learning approach that decodes the grasping intention at an early stage of reach-to-grasp motion, i.e. before the final grasp/hand pre-shape takes place. Superficial electrodes and a Cyberglove were used to record the arm muscle activity and the finger joints during reach-to-grasp motions. Our results showed a 90% accuracy for the detection of the final grasp about 0.5 s after motion onset. This paper also examines the effect of different objects' distances and different motion speeds on the detection time and accuracy of the classifier. The use of our learning approach to control a 16-degrees of freedom robotic hand confirmed the usability of our approach for the real-time control of robotic devices.

© 2017 Elsevier B.V. All rights reserved.

1. Introduction

Nowadays, robotic devices are frequently used to restore motor abilities lost after pathologies or trauma, such as exoskeletons and operative devices adopted for the patient's assistance during rehabilitation, and the prostheses for amputees [1]. Studies on amputees and stroke patients [2,3] have reported that comfort is one of the priorities for the acceptability of a wearable robotic device, and that inconvenient and time ineffective systems may avert individuals from using a prosthetic device [2]. To increase the level of comfort and effectiveness, these devices should detect the human intention early enough in order to ensure the smooth and prompt behavior of the system.

It has been extensively demonstrated that user's motion intention can be accurately detected by surface electromyographic recordings (sEMG) [4]. Different sEMG-based systems were proposed for the estimation of hand and wrist movements, and consequently used as noninvasive interfaces for controlling exoskeletons [5,6], prosthetic devices [7–9], computer-animated hands in a virtual environment [10], or for teleoperating robotic arms [9,11]. The previous studies focused on the investigation of discrete classifications of wrist abduction/adduction [9,11], flexion/extension [7,10,12,13] as well as of a different combination of finger motions [9,11,14]. Such strategies are useful for accomplishing power grasps that require simultaneous closure of all fingers on the object. However, this is insufficient to generate differentiated control of all fingers in the variety of pinch grasps used in dexterous objects manipulation, as required by the grasping of a larger variety of objects.

The differentiated control of all fingers is complex to achieve due to the high dimensionality of the hand's degrees of freedom.

* Corresponding author.
E-mail addresses: iason.batzianoulis@epfl.ch (I. Batzianoulis), sahar.elkhoury@epfl.ch (S. El-Khoury), elvira.pirondini@epfl.ch (E. Pirondini), martina.coscia@epfl.ch (M. Coscia), silvestro.micera@epfl.ch (S. Micera), aude.billard@epfl.ch (A. Billard).

Indeed, the human hand is characterized by 21 degrees of freedom (DOFs) controlled by 29 muscles [15]. It has been hypothesized that humans are capable to control this large number of DOFs and use their hands dexterously thanks to a multidimensional reduction of the controlled variables operated by the central nervous system. This multidimensional reduction may be accomplished through the use of postural synergies [16] , corresponding to a number of hand postures that humans combine when grasping everyday life objects. Several works propose to exploit a mapping between upper limb EMG signals and hand postures [17–20], as strategy to control the large number of the hand's degrees of freedom. However, in these approaches only the grasping phase, i.e. when the fingers have already reached their final configuration, was examined and the subjects were asked to perform the corresponding grasp keeping the upper-arm stalled. Nonetheless, the muscular activity differs between a static and a dynamic position of the arm. Moreover, during reaching-to-grasp movements, the configuration of the fingers and of the wrist changes simultaneously with the arm's motion and this might influence the classification performance. This formation of the fingers, before reaching their final configuration, is defined as hand's preshape. The preshape of the hand is in direct relation with the characteristics of the object, specifically to the shape and width of it. In healthy human subjects, the hand's preshape occurs before the hand reaches the object, at around 60% of the reach and grasp motion [21–24]. Therefore, in order to accomplish a smooth control of the grasping gesture, it seems is crucial to classify the hand posture during the reaching phase before the occurrence of the preshape. Indeed, an accurate estimation of the final grasp posture in the early stages of the reach-to-grasp motion would ensure a faster reactivity of the assistive and the wearable devices. As result, these devices would increase their effectiveness and usability, and consequently increase the natural transition between the reaching and grasping phase on the prostheses increasing their acceptance by patients. However, at the moment only a limited number of studies focused on the detection of different grasp movements during reaching and grasping motions [25–27], and no measurement were performed to assess when a good classification was achieved respect to the hand's preshape .

In this work we propose a new sEMG-based learning approach that decodes the grasping intention of the user at an early stage of the reach-to-grasp motion, i.e. before the final grasp/hand preshape takes place. We demonstrate as well the extensibility of our work to online applications. The rest of this paper is organized as follows. Section 2 describes the experimental set-up, protocol and methods used to record and analyze the data, while Section 3 reports the results of the experiments. In Section 4, the online robotic implementation is presented. In Section 5, we discuss the results of the experiment and the future perspectives.

2. Methods

2.1. Participants

Fourteen healthy young subjects (10 males and 4 females, average age 28.2 ± 3.9) participated in the experiment. All subjects were right handed according to the Edinburgh inventory test [29], and they had no prior history of neurological disorders and neuromuscular injuries. They performed the experiments with their dominant arm. The experiment was approved by the BMI Ethics Committee for Human Behavioral Research of the EPFL, and the recordings were carried out in agreement with the Declaration of Helsinki. All subjects gave written consent to the participation at the beginning of the experiment.

2.2. Experimental protocol

The subjects were asked to reach and grasp 3 different objects, accounting for five different grasp types: precision disk, tripod, thumb-2 fingers, thumb-4 fingers, and ulnar pinch, see Table 1. These grasps were mostly chosen for their common usage in daily life [28].

During the experiment, the subjects seated in front of a table with the elbow flexed of about 90° and the hand placed on the table with the palm downward and the fingers pointing to the object, see Fig. 1(a). The subjects were asked to reach the object and grasp it with a predefined grasp type keeping the same hand's orientation for all the grasp types. The subjects were starting the self-paced motion after the advice of the experimenter and they had to declare that they grasped the object in order to consider the trial completed. The objects were placed at three different distances (i.e., 30 cm, position P1, 20 cm, position P2, and 10 cm, position P3) from the initial hand's position, see Fig. 1(b). All the fourteen subjects performed 20 trials for each of the five grasp types for position P1. After completing this first part of the experiment, six subjects continued the experiment for the positions P2 and P3 performing 15 trials for each grasp type. In addition, three subjects performed additionally fast reach-to-grasp motions for objects placed at position P1, asked to perform the motions by extending their arm with higher acceleration than the first part of the experiment. The subjects were performing all trials for one grasp before moving to the next grasp.

2.3. Apparatus and pre-processing

The EMG signals from 16 upper limb muscles (Table 2), were recorded using a Noraxon DTS desktop system, with a sampling rate of 1500 Hz. The electrodes were placed, when it was possible, according to the standard procedure for surface electromyography for non-invasive assessment of muscles (SENIAM) guidelines [30]. At the beginning of the recordings, a manual test for the maximum voluntary contraction (MVC) was performed for each muscle. During the test, the subjects were asked to perform isometric contractions for each muscle. The test was repeated three times for each muscle, with a break after each contraction to prevent muscle fatigue.

The data were filtered with a seventh-order band-pass Butterworth filter between 50 Hz and 500 Hz for the suppression of movement artifacts. To construct a linear envelope, full-wave rectification was performed, followed by a smoothing with a low-pass seventh-order Butterworth filter with cutoff frequency at 20 Hz. Finally, the resulting EMG signals were normalized by the MVC.

The joint angles of the fingers were measured using CyberGlove System's CyberGlove,[1] with a sampling rate of 280 Hz. The Cyberglove has 22 bend sensors strategically located over the hand joints. Since bending can be detected anywhere along the sensor length, the glove can adapt well to different hands sizes and it needs to be calibrated in order to transform raw sensor values to hand joint angles. Linear regression was used to calibrate the 4 fingers (index, middle, ring, and little) while a data-driven approach was employed to model the non-linear relationship between the thumb sensors and the joint angles. The recorded joint angles were used to compute the fingertip's position with respect to the wrist by forward kinematics. More details about the Cyberglove calibration procedure could be found in [31].

The two data streams were synchronized using a trigger signal provided by an Arduino board. At each trial, the subjects were starting the motion once instructed to do so by the experimenter.

---

[1] www.cyberglovesystems.com.

Table 1
Chosen grasp types [28].

	Precision disk	Tripod	Thumb-2 fingers	Thumb-4 fingers	Ulnar pinch
Grasp types					
Fingers involved	5 (all fingers)	3 (thumb, index, middle)	3 (thumb, index, middle)	5 (all fingers)	2 (thumb and little finger)
Object	Large cylinder (10 cm diameter)	Small cylinder (5 cm diameter)	Thin rectangular	Thin rectangular	Thin rectangular
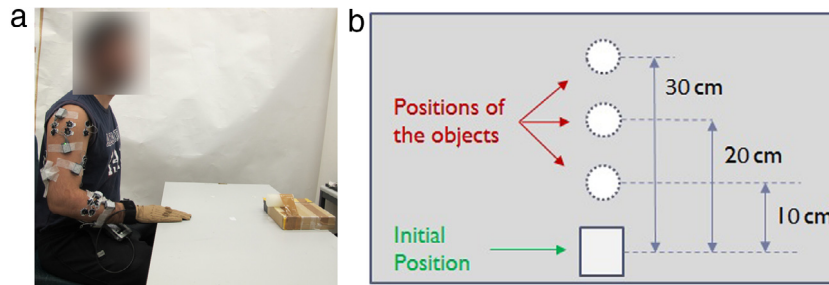
Fig. 1. (a) The experimental setup showing the electrodes for EMG recording and the CyberGlove for capturing the hand joint angles, (b) the plan showing the initial position of the hand and the three positions of the object.

Table 2
Muscles which activity is captured for the reaching and grasping experiment.

	Muscles
1	Infraspinatus (INFRA)
2	Deltoid Anterior (DANT)
3	Deltoid Medial
4	Deltoid Posterior (DPOS)
5	Biceps Brachii long head (BICL)
6	Triceps Brachii long head (TRIC)
7	Brachialis (BR)
8	Flexor Digitorum Superficialis (FLDS)
9	Extensor Digitorum Communis (EXDC)
10	Flexor Carpi Ulnaris (FLCU)
11	Extensor Carpi Ulnaris (EXCU)
12	Flexor Carpi Radialis (FLCR)
13	Flexor Pollici Brevis (FLPB)
14	Extensor Pollicis Brevis (EXPB)
15	AdductorPollicis Transversus (ADPT)
16	AbductorDigiti Minimi (ABDM)

Simultaneously, the experimenter was pressing a button in the console, which was generating a trigger pulse, indicating the start of the recording of the Cyberglove data. The trigger pulse was introduced to the Noraxon system as an extra channel. During the offline analysis, all the data were synchronized with respect to the trigger pulse, ensuring the synchronization between the Cyberglove and the Noraxon system. The onset of the motion was detected from the joint angles of the fingers, as they were switching from rest position to motion generation. This transition results into a change on the angular velocity of the joint angles of the fingers, which is captured by the Cyberglove and corresponds to the moment $t = 0$ s on the analysis and the figures.

2.4. Preshape criteria

As stated previously, the preshape of the hand is considered as the formation of the fingers before they reach their final configuration [32]. In this work, we employed two criteria to identify the occurrence of the hand preshaping [21,33]. The first criterion was based on the distance between the fingertips of the thumb and the index finger, which are considered the fingers participating in most of the grasp types. For this reason they provide valuable information for the configuration of the fingers and more particularly for the opening and closing of the hand. In the case of the ulnar pinch, which is performed with the thumb and little finger, we replaced the index finger with the little finger. The first criterion is defined in the literature as the hand's aperture and in this paper we will refer to it as *aperture*.

The second criterion was based on the estimation of the area of the polygon that is described by the fingertips involved in the grasp. For the precision disk and the thumb-4 fingers, the area considered was the one of the pentagon created by the fingertips of all five fingers. For the tripod grasp and the thumb-2 fingers, the area was the surface of a triangle defined by the fingertips of the thumb, index, and middle finger. Finally, for the ulnar pinch, the area was again the surface of a triangle but consisted of the fingertips of the thumb, the index finger, and the little finger. In the following section we will refer to this criterion as *area*.

To estimate the *aperture* and the *area*, we computed the position of the fingertips with respect to the wrist,using the joint angles of the fingers, recorded from the Cyberglove. The *aperture* and the *area* vary with respect to the opening and closing of the hand, providing objective information for the determination of the preshaping. In particular, the preshaping was assumed to correspond to the peak value of the aperture and the area while the grasp is considered complete when these criteria reach stability.

2.5. Classification method

The preprocessed EMG signals were analyzed using a sliding time window of 150 ms with an overlap of 50 ms. In order to embed the specificity of the motion's time evolution, we combined an Echo State Network (ESN) [34] to classify the data with the Majority Vote (MV) criterion applied to each time window from the motion onset, as suggested in [35]. The MV criterion assigns a class label to the class that gathers the most votes. The preprocessed EMG data input were provided as input to the ESN, without extracting any feature from the EMG signals. Each ESN entailed 180 sigmoid

units, with a transfer function $f = \tanh$, and it outputted 5 classes for each of the 5 grasp types. Moreover, the activation function of the output units was chosen to be the identity function. The classification for each time window was fed to the MV algorithm, where each vote corresponded to the result of the classification.

Since the classification strategy is implemented online, the following analysis was performed in the time domain, avoiding time normalization. As the hand's preshape occurs around the 60% of the reaching motion, we chose to analyze the first second of the reaching motion. This approach enables the capture of the hand's preshape in different time steps and its the relation with the classification rates.

One classifier was trained for each subject. For the first position of the object (P1), the classification machine was built with the 75% of the dataset of 100 trials (i.e., training dataset) and tested in the remaining data (i.e., 25%) using the cross-validation method. For the generalization over different distances (i.e., positions P2 and P3), two different classifiers were built. In the first case, the training dataset was constituted by the data from two different positions, and the testing dataset included only the data from the remaining positions. In the second case, instead, the classifier was trained on one position and tested in the other two.

Moreover, in the case of the trials at different speeds, we tried different combination of training and testing data in order to examine the performance of generalization. First, the classifier was trained with data of self-paced motions and tested with data on fast motions. As a second step, the classification machine was trained with data of fast motions and tested with data of self-paced motions. In the last test, we mixed the data of fast and slow motions while the classification machine was trained with 75% of the data and tested with the remaining 25%, following a four-folder cross-validation.

Additionally, we examine the performance of the approach with less number of EMG channels as input to the classifier. We first removed the intrinsic muscles of hand *(Abductor Digiti Minimi, Adductor Pollicis Transversus* and *Flexor Pollici Brevis)*, keeping 13 EMG channels. As a second step, we excluded the activity of the *Extensor Pollicis Brevis* which contributes to the flexion and abduction of the thumb, which left us with 12 EMG sites. Moreover, we remove the activity of the *Flexor Carpi Radialis* and the ulnar muscles (*Flexor Carpi Ulnaris* and *Extensor Carpi Ulnaris*) keeping 11 and 9 EMG channels accordingly. Finally, we kept only the 7 EMG muscles that correspond to muscles from the upper arm (i.e *Infraspinatus, Deltoid Anterior, Deltoid Medial,Deltoid Posterior, Biceps Brachii long head, Triceps Brachii long head* and *Brachialis*).

2.6. Online robotic implementation

For the purposes of the online implementation, we used a right Allegro hand from Simlab.[2] This is a humanoid hand with 16 DOF split equally on 4 fingers. While it is only an approximate reproduction of the dexterity of the human hand and it has more DOFs than currently available assistive devices, it serves as a benchmark for our ability to reproduce grasps with similar dexterity to those generated by humans. The Allegro hand has also the advantage to be controlled at an extremely fast rate (400 Hz) that enables demonstrating the benefit of our early pre-shape detection for real-time control of finger closure during the arm movements.

In the online robotic implementation, the EMG signals were acquired using a National Instruments USB-6210 data acquisition board with a sampling rate at 1000 Hz. The acquired signals were pre-processed (filtered and rectified as described in previous subsection) and classified using a C++ project of Visual Studio 2013 installed in a desktop computer (Intel Xeon @ 2.27 GHz with
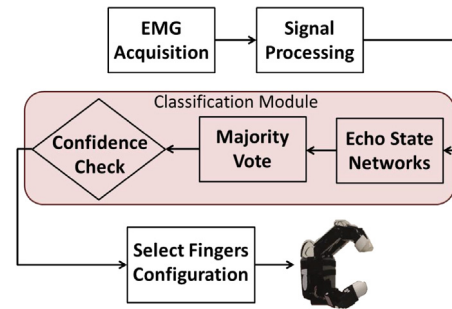

Fig. 2. Control scheme of the robotic implementation.

Windows 8.1). The classification output for each time window was streamed to a portable computer (Intel i7 @ 2.6 GHz with Ubuntu 14.01) and introduced to the majority vote algorithm. Finally, the corresponded joint angles were imported to the Allegro hand using ROS. The straight forward control scheme is presented in the Fig. 2).

3. Results

In order to assess the classification accuracy and the robustness of the results, we defined the success rate as the percentage of movements correctly classified for a specific grasp type on the total number of reach-to-grasp motions corresponding to that specific grasp type (Recall column in Table 3). We also computed the precision measure (i.e., the percentage of trials correctly classified for a specific grasp type on the total number of reach-to-grasp movements classified to the same grasp type) and the F-measure, which corresponds to the harmonic average of the recall and precision values, for each grasp type. An F-measure score of 1 means that each motion belonging to a specific grasp type was perfectly classified as such. After presenting the Recall, Precision and F-measure values of each time window, we define the classification performance as the number of correctly classified trials over the total number of trials, for simplicity purposes.

3.1. Reach-to-grasp classification strategy

Table 3 shows the average and standard deviation of the classification results across subjects and grasps for 10 different time windows starting from 0.15 to 1.05 s with a step size of 100 ms. The average classification performance among subjects increased during time, as the hand was getting closer to the object (see Fig. 3(b)) for all the three positions with a slight decrease only at 450 and 950 ms for P1 (see Table 3. In particular, a success rate of $90 \pm 4.5\%$ was reached 0.5 s after motion's onset (i.e., half-way through the reaching motion). On average, a F-measure of 0.91 was obtained for the five grasp types and for all time windows. However, it was higher than 0.76 already 150 ms after motion onset, showing that an accurate classification of the five grasp types was possible before the grasp occurred.

Fig. 3(a) shows the confusion matrix averaged across subjects for the five grasp types 550 ms after motion onset. This timing was chosen because it corresponded to half-way of the reach-to-grasp motion. Precision disk, tripod and ulnar pinch were distinguishable already at half motion (89.5%, 92.7% and 98.3% respectively), while thumb-2 fingers and thumb-4 fingers were distinct later in the reaching motion when the hand was closer to the object (85.1% for both of the classes). As expected from the hand configuration during the grasping, a misclassification tended to occur between tripod and precision disk and between thumb-2 and thumb-4
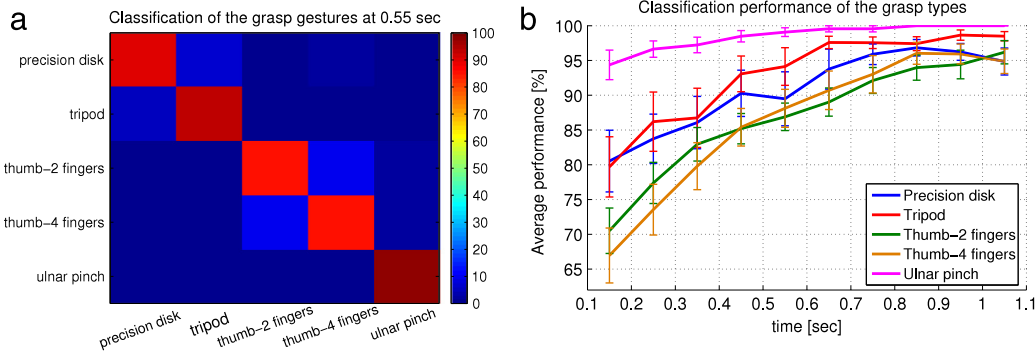
Fig. 3. (a) Confusion matrix of the classification between grasp types in among the subjects, 0.55 s after the onset of the motion. Warmer color indicates higher classification performance, (b) Average and standard error of the classification performance of all the grasp types among subjects for 30 cm distance of the object. (For interpretation of the references to colour in this figure legend, the reader is referred to the web version of this article.)

Table 3
The average and standard deviation of the classification results across grasp types and subjects. The *Recall* values correspond to the percentage of EMG data correctly classified as a specific grasp type to the total number of reach-to-grasp motions corresponding to the same grasp type. The *Precision* values correspond to the percentage of EMG data correctly classified as a specific grasp type to the total number of reach-to-grasp motions classified to the same grasp type. The *F-measure* values corresponding to the harmonic average of the recall and precision values. The last row of each of the above tables correspond to the total average across time windows.

Time (s)	ESN MV		
	Precision	Recall	*F*-measure
0.15	0.81 ± 0.06	0.84 ± 0.05	0.76 ± 0.08
0.25	0.89 ± 0.04	0.91 ± 0.04	0.88 ± 0.05
0.35	0.87 ± 0.06	0.89 ± 0.06	0.84 ± 0.06
0.45	0.93 ± 0.04	0.94 ± 0.04	0.92 ± 0.04
0.55	0.91 ± 0.06	0.92 ± 0.05	0.90 ± 0.06
0.65	0.95 ± 0.02	0.96 ± 0.02	0.94 ± 0.03
0.75	0.95 ± 0.03	0.95 ± 0.03	0.94 ± 0.03
0.85	0.97 ± 0.02	0.97 ± 0.01	0.96 ± 0.02
0.95	0.96 ± 0.03	0.97 ± 0.02	0.95 ± 0.03
1.05	0.97 ± 0.02	0.98 ± 0.01	0.96 ± 0.02
Total av.	0.92	0.93	0.91

Table 4
The results from the pairwise comparison of the classification performances, 0.55 s after the onset of the motion, when using different muscle groups. The highlighted cells depict the pairs in which the null hypothesis was not rejected at the significant level of 5%.

p values, $t = 0.55$ s after the motion onset

	16	13	12	11	9
13	0.9435				
12	0.4039	0.9157			
11	0.3743	0.8981	0.9989		
9	0.0004	0.0087	0.1276	0.1424	
7	$< 10^{-3}$	$< 10^{-3}$	$< 10^{-3}$	$< 10^{-3}$	0.0243

fingers (85.5% and 85.8% respectively). From Fig. 3(b), we notice that thumb-2 fingers and thumb-4 fingers are reaching 90% of classification rate 0.7 s after the onset of the motion.

3.2. Decreasing the number of EMG channels

In this subsection, we examine the performance of the approach when using a smaller number of EMG sites, by removing the more distal muscles. As previously stated, for this analysis we kept 13, 12, 11, 9 and 7 muscles from the initial muscle set as input to the classifier.

Fig. 4 presents the evolution through time of the classification success rates. As depicted the classification performance decreases
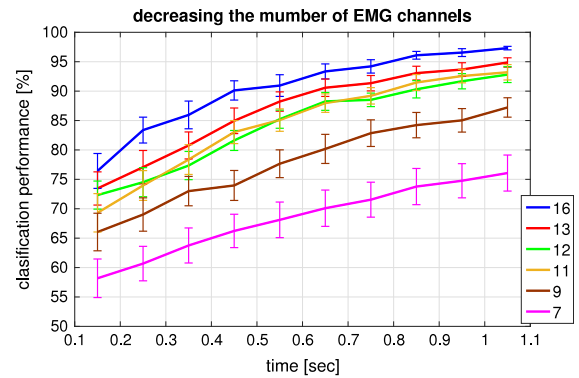

Fig. 4. The evolution of classification performance and its standard error while reducing the number of EMG sites. The object was 30 cm away from the initial position of the hand.

Table 5
The results from the pairwise comparison of the classification performances, 1.05 s after the onset of the motion, when using different muscle groups. The highlighted cells depict the pairs in which the null hypothesis was not rejected at the significant level of 5%.

p values, $t = 1.05$ s after the motion onset

	16	13	12	11	9
13	0.9007				
12	0.3921	0.9493			
11	0.4977	0.9798	0.9989		
9	0.0006	0.0189	0.1715	0.1188	
7	$< 10^{-3}$	$< 10^{-3}$	$< 10^{-3}$	$< 10^{-3}$	0.0001

as the number of muscles becomes smaller. The success rate at $t = 0.55$ s (0.55 s after the onset of the motion) is between $90.95 \pm 1.85\%$ and $85 \pm 1.9\%$ when using more than 10 muscles, and drops rapidly to $77.65 \pm 2.36\%$ and $68.95 \pm 3.03\%$ when using 9 and 7 muscles respectively.

The one-way analysis of variance (ANOVA) performed on the classification performances rejected the null hypothesis at the significant level of 5% ($p < 10^{-3}$ for $\alpha = 0.05$). The Tables 4 and 5 present the results of the pairwise comparison analysis of the classification performances at the moment of $t = 0.55$ s and $t = 1.05$ s. As it is shown, the performance decreases significantly when reducing the number of EMG channels from 16 to 9 while it is not significantly different when using 13, 12 and 11 muscles. Additionally, a significant drop in performance was observable when using 9 and 7 muscles.
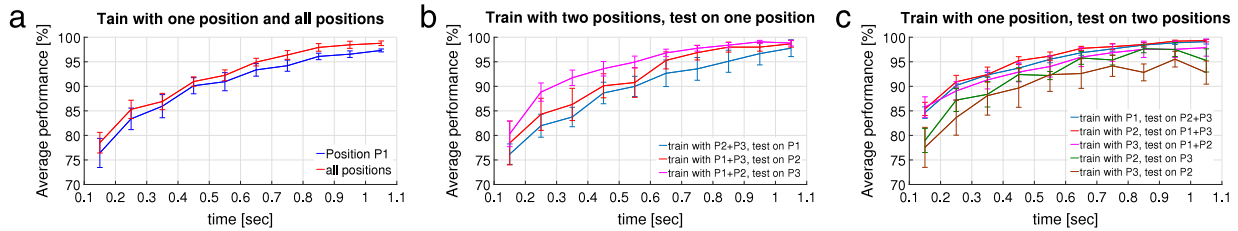
Fig. 5. Classification success rate in different distances: (a) Average classification performance and standard error on the reaching motion: The blue line presents the performance of the classification of grasp types on position P1. The red line corresponds to the classification performance when all the positions (P1, P2 and P3) are taken into account, (b) Average classification performance and standard error on training with two positions and testing on the third: The blue line presents the performance when training on reaching motions to two positions P2 and P3 and testing on position P1. Respectively, the red line corresponds to training on positions P1 and P3 and testing on position P2 while the magenta line corresponds to training on positions P1 and P2 and training on position P3, (c) Average classification performance and standard error on training with one position and testing on the other two positions: The blue line presents the performance when training with reaching motions to positions P1 and testing on positions P2 and P3. Respectively, the red line corresponds to training on position P2 and testing on positions P2 and P3, while the magenta line corresponds to training on positions P3 and training on position P1 and P2. The green line corresponds to training with position P2 and testing on position P3. The brown line corresponds to training with position P3 and testing on position P2. (For interpretation of the references to colour in this figure legend, the reader is referred to the web version of this article.)
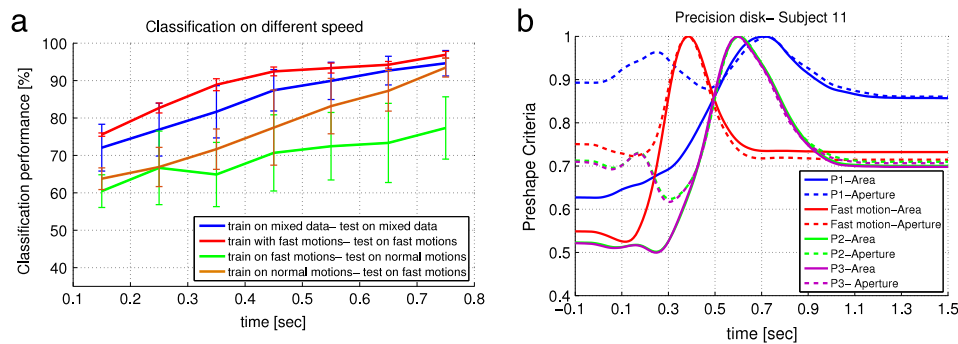

Fig. 6. (a) Average classification performance and standard error on the fast motions: The red line presents the performance of the classification of grasp types with the data of fast motions. The blue line corresponds to the classification performance when the data of fast motions were mixed with the data of normal motions. The green line corresponds to the performance when training with fast motions and testing on normal motions. The brown line corresponds to the performance when training with normal motions and testing on fast motions. the magenta and cyan vertical lines indicate the peak of the preshape criteria then subject 11 performed the precision disk grasp with fast and normal motions respectively as depicted in Fig. 6(b). (b) Preshape criteria on the precision disk of subject 11: The subject opens its fingers sooner in fast motions than it does in normal motions. (For interpretation of the references to colour in this figure legend, the reader is referred to the web version of this article.)

3.3. Generalization on different distances

As second step, we examined the generalization across distances by (i) training the classifier on two positions (i.e., P1 and P2 or P1 and P3) and testing it on the remaining third position (P3 or P2, respectively) and, (ii) training the classifier on one position (i.e., P1 or P2 or P3) and testing it on the other two (i.e., P2 and P3 or P1 and P3 or P1 and P2, respectively). The performances were higher when the classifier was trained with a single position with respect to a classifier trained on two positions (see Figs. 5(b) and 5(c)). Indeed, the average performance at 0.45 s after movement onset was $93.93 \pm 1.7\%$ and $90.78 \pm 2.5\%$ when training on one position and on two positions, respectively. For the classifier trained with two positions, the performance was better when the training set included movements from farthest distances (i.e., P1 and P2) and the testing set included the shortest distance (i.e., P3) (see Fig. 5(b)). The performance in this case was $93.6 \pm 3.6\%$ after 0.45 s from the motion on set. For the classifier trained with a single position, instead, the best classification performance was achieved when the classifier was trained in the middle distance (i.e., P2) and tested on the other two distances (i.e., P1 and P3) (see Fig. 5(c)). In this case, a classification accuracy of $95.2 \pm 2.0\%$ was achieved 0.45 s after movement onset. It is worth mentioning that this case (i.e., training with P2 and testing on P1 and P3) presented as well the smallest standard error when compared to the other generalizations. An one-way analysis of variance on the classification performance at the moments $t = 0.55$ s and $t = 1.05$ s after the onset of the motion failed to reject the null hypothesis on the significant level of 5% ($p = 0.12$ and $p = 0.88$ respectively).

3.4. Speed effect

In order to further evaluate the generalizability of our approach, we examined the effect of the speed on the classification. We first analyzed the differences in fingers' motion in fast movements with respect to self pace motions. As expected there was a significant difference on the timings of hand opening and closing between motions performed at self-paced speed and at fast speed (see Fig. 6(a)). Indeed, the subjects opened and closed their hand in fast motions sooner in time than in self-paced motions.

As first step, we mixed the data at self pace and during fast motions for training and testing. The classification performance reached $90 \pm 2.3\%$ of success after 0.55 s from movement onset. We then compared this first classification with the results obtained training the classifier in the fast motions and testing it in either for the fast or self pace motions, or training the classifier with the movements at self-selected speed and testing it for the fast motions. As expected when using only data from the fast motions both for training and testing, the classification performance reached an accuracy higher than 90% earlier than when mixing the movements (0.35 s for fast motions, 0.55 s for self-paced motions). On the contrary, the classifiers trained and tested in different datasets achieved lower performances than that trained and tested with mixed data. In particular, the accuracy of 90% was achieved 0.7 s after motion onset. Moreover, the standard error of these classifiers was higher than 4.5%, which indicated that the classifier performed significantly better in some subjects than in others.

Table 6
The average times and standard deviations of the preshape occurrence per grasp type.

	$P1 = 30$ cm	$P2 = 20$ cm	$P3 = 10$ cm	*Fast*
Precision disk	0.74 ± 0.17 s	0.62 ± 0.18 s	0.52 ± 0.24 s	0.40 ± 0.25 s
Tripod	0.71 ± 0.24 s	0.60 ± 0.17 s	0.56 ± 0.25 s	0.53 ± 0.21 s
Thumb-2 fingers	0.53 ± 0.28 s	0.48 ± 0.24 s	0.47 ± 0.24 s	0.38 ± 0.19 s
Thumb-4 fingers	0.38 ± 0.2 s	0.31 ± 0.22 s	0.30 ± 0.23 s	0.42 ± 0.22 s
Ulnar pinch	0.43 ± 0.21 s	0.42 ± 0.23 s	0.42 ± 0.25 s	0.41 ± 0.12 s

Table 7
The average times and standard deviations of the preshape occurrence and task completion on the different motions.

	Preshape occurrence	Completion time
$P1 = 30$ cm	0.56 ± 0.26 s	1.30 ± 0.27 s
$P2 = 20$ cm	0.49 ± 0.21 s	1.19 ± 0.22 s
$P3 = 10$ cm	0.46 ± 0.25 s	1.14 ± 0.25 s
Fast	0.40 ± 0.11 s	0.83 ± 0.17 s

Table 8
The results from the pairwise comparison between the timings of the preshape occurrence. The highlighted cells depict the pairs in which the null hypothesis was not rejected at the significant level of 5%.

preshape occurrence			
	30 cm	20 cm	10 cm
20 cm	10^{-3}		
10 cm	$< 10^{-3}$	0.91	
Fast	$< 10^{-3}$	$< 10^{-3}$	$< 10^{-3}$

Table 9
The results from the pairwise comparison between the task completion times. The highlighted cells depict the pairs in which the null hypothesis was not rejected at the significant level of 5%.

completion time			
	30 cm	20 cm	10 cm
20 cm	10^{-3}		
10 cm	$< 10^{-3}$	0.21	
Fast	$< 10^{-3}$	$< 10^{-3}$	$< 10^{-3}$

3.5. Classification rate vs hand preshape

To quantify how early into the preshape phase, we could detect the grasp intention, we used two criteria: (a) the hand *aperture*: the distance between the fingers involved during the grasp (i.e., thumb and index finger for Precision disk, Tripod, Thumb-2 fingers and Thumb-4 fingers and thumb and pinky finger for Ulnar pinch grasp) and (b) the *area* of the fingertips: the surface obtained interconnecting the tips of the fingers involved in each grasp.

It is worth mentioning that the aperture involves solely the behavior of the thumb and index finger. Thus, the area criterion could be more informative of the motion of the fingers, as it encapsulates the behavior of all the fingers involved in the grasp [33]. In order to examine the general trends of the motion of the fingers, we computed the two criteria in normalized time and present the results in Fig. 7. As it is shown, the preshape is indicated in three grasp types (*precision disk, tripod* and *thumb-4 fingers*) by the peak of the *area* criterion which is followed by a smooth convergence to the final point. In the case of the *thumb-4 fingers* grasp, the start of the preshape phase is also revealed through a peak in the aperture, that occurs simultaneously with the peak of the *area* criterion. Both curves then decrease smoothly until full closure onto the final grasp. In the case of *thumb-2 fingers* grasp, it is more difficult to define the moment of preshape occurrence (see the third graph of Figs. 7(a) and 7(b)), as the fingers begin their motion with a flexion until the 30%–40% of the duration of the self-paced motions. At this point, the value of the area criterion stays approximately stable for a period of time before closing smoothly to the final grasp. In the same period, the value of the aperture criterion decreases, indicating a flexion of the index finger and the thumb. As the thumb-2 fingers grasp involves the middle finger too, the area criterion encapsulates the behavior of the middle finger. In order for the value of the *area* criterion to stay stable while the index finger and the thumb are flexing, the middle finger extends until all the fingers start to close simultaneously. We considered that the preshape occurs when the *area* criterion starts converging smoothly to its final value. Regarding the ulnar pinch, two fingers are involved, the thumb and the little finger. In this case, the *aperture* criterion, which corresponds to the distance between the fingertips of the thumb and the little finger, is more representative of the preshape than the *area* criterion, which involves more fingers. Thus, we considered that the preshape occurs on the peak of the *aperture* criterion. Fig. 8 presents the fingers configuration on the initial hand position, on the preshape and in the end of the motion.

Table 7 presents the average real time of preshape occurrence as well as the completion time for all the motions. The one-way analysis of variance (ANOVA) rejected the null hypothesis at a sig-

nificant level of 5% for the preshape occurrence and the completion time ($p < 0.001$ for $\alpha = 0.05$). A pairwise comparison analysis of the timings of the preshape and task completion showed that the timings are not significantly different between the self-paced motions when the object is placed 20 cm and 10 cm away of the initial position of the hand (Tables 8 and 9).

After examining the behavior of the fingers, we extracted the timings of the preshape occurrence with a visual inspection of the criteria for each trial. The average and standard deviation of the time of the preshape occurrence and completion time are presented in Table 7. As it is shown the preshape occurs in average between 0.46–0.56 s after the onset of self-paced motions. Fig. 5(a) presents the evolution of the classification performance through real time. As it is shown, the success rate reaches a 90% of classification accuracy, as an average, at 0.45 s after the onset of the self-paced motions. These results suggest that it possible classify the grasp type during the preshape of the fingers.

We also compared the classification performance with the preshape occurrence for each grasp type individually. Table 6 presents the time of the preshape occurrence for all the grasp types while Fig. 3(b) presents the evolution of the classification performance for all grasp types in real time. Comparing the time preshape occurrence from Table 6 with the classification results of the Fig. 3(b), we notice that the success rate for the precision disk reaches $89.5 \pm 3.8\%$ of accuracy 0.55 s after the onset of the motion while the corresponding preshape appears 0.74 ± 0.17 s after the motion onset. Concerning the tripod grasp, a $94.1 \pm 2.7\%$ of classification accuracy is observed at 0.55 s while the preshape occurs at 0.71 ± 0.24 s after the motion onset. Continuing with the thumb-2 fingers grasp type, a $92.1 \pm 1.8\%$ of classification accuracy is noticed 0.75 s after the onset of the motion, while the corresponding preshape occurs 0.53 ± 0.28 s after the motion onset. Regarding the thumb-4 fingers, a $90.7 \pm 2.8\%$ of classification accuracy is noticed 0.65 sec after the onset of the motion, while the corresponding preshape occurs 0.38 ± 0.20 s after the motion onset. Finally about the
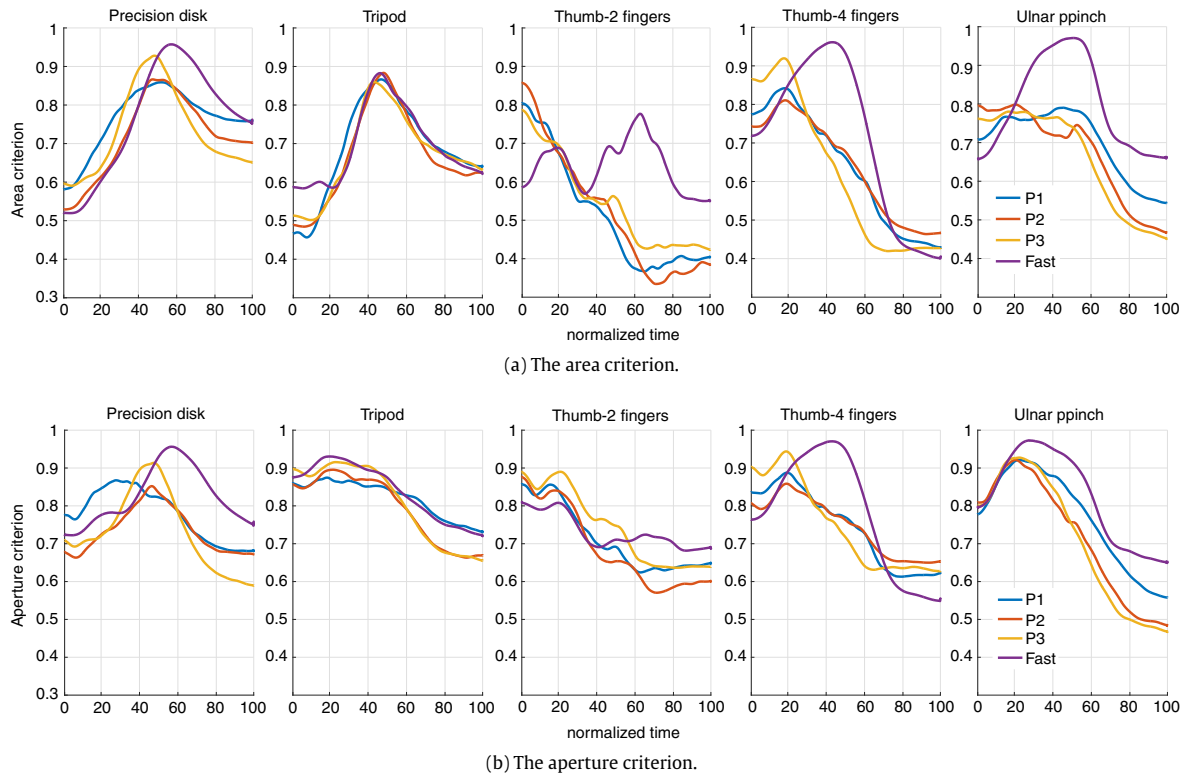
(a) The area criterion.

(b) The aperture criterion.

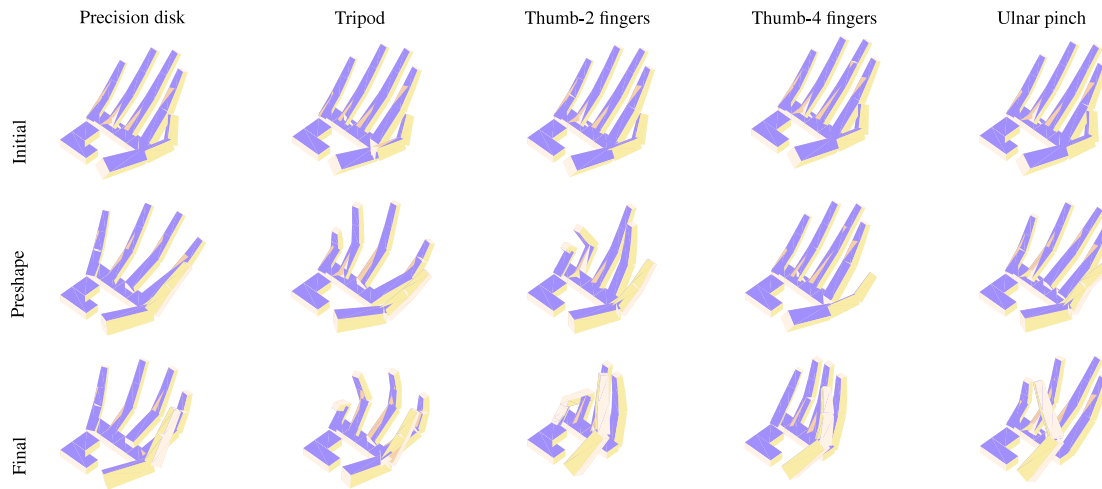**Fig. 7.** The average value of preshape criteria across all subjects.

Fig. 8. Configuration of the fingers in three different moments of the reaching motion: Initial configuration (before the onset of the motion), configuration on the preshape, final configuration (when grasping the object).

ulnar pinch, a $94.46 \pm 2.1\%$ of classification accuracy is noticed 0.15 s after the onset of the motion, while the corresponding preshape occurs 0.43 ± 0.28 s after the motion onset. In summary, it is noticed that 90% of classification performance is achieved before the preshape occurrence for three grasp types (precision disk, tripod and ulnar pinch) while for the other two the preshape preceded the 90% of classification accuracy.

3.6. Online robotic implementation

In order to demonstrate the usability of the proposed approach for the estimation of the final grasp gesture in the early stages of the reaching motion for an assistive or a rehabilitative application, we present here an online robotic implementation of our approach.

The system was trained offline while the testing was performed online using the aforementioned control scheme of the Fig. 2). We had defined a set of desired joint configuration for the Allegro hand's 4 fingers so that these correspond to similar postures to the human hand, see Fig. 10. As soon as the classifier had reached the confidence threshold of 0.5, the fingers of the robotic hand were driven to their desired final posture. The confidence of the majority vote was defined as the difference in votes of the winner from the second winner divided by the sum of all the votes.

Five able-bodied subjects participated in the online implementation experiment(four males and one female). The subjects performed 15 self-paced reach-to-grasp motions for each grasp type with the objects placed 30 cm away from the initial position of the hand. The recorded dataset consisted of 75 trials was used to train
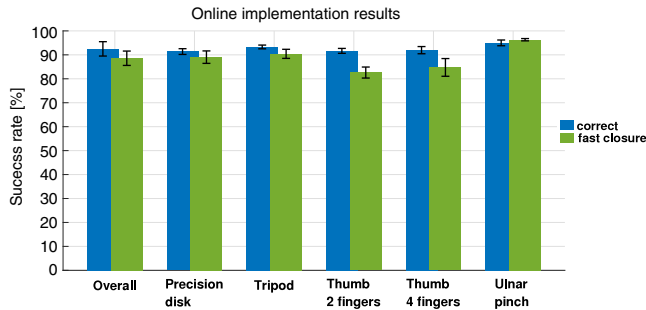
Fig. 9. Online implementation results.

Table 10

The activation times of the robotic hand for all grasp types in the online implementation. The third column of the table corresponds to time needed for the robotic hand to take its final configuration closing with its maximum velocity.

Grasp type	Activation time	Closure
Precision disk	0.53 ± 0.13 s	0.32 s
Tripod	0.54 ± 0.16 s	0.41 s
Thumb-2 fingers	0.58 ± 0.25 s	0.41 s
Thumb-4 fingers	0.63 ± 0.30 s	0.42 s
Ulnar pinch	0.54 ± 0.12 s	0.41 s

the system offline. After the training phase, the subjects performed 30 reach-to-grasp motions for different objects, using a grasp type of their choice, between these five grasp types. The results of the online implementation are presented on the Fig. 9. The 92.5 ± 2.9% of the test trials were successful allowing the execution of the correct grasp type. In the 88.58 ± 3% of the successful trials the robotic hand reached its final configuration before the subject reached the object (see the video to lasa.epfl.ch/~sina/Demo.mp4 and Fig. 10). Moreover, all the grasp types have an average success rate above 90% at the end of the motion and above 80% on the early prediction of the grasp type. The lowest performances on the early prediction appear at the *thumb-2 fingers* and *thumb-4 fingers* grasp types with 82.6 ± 4.3% and 84.75 ± 3.7% respectively. The highest performances on the early prediction of the grasp type was noticed at the *ulnar pinch* (96.3±0.5%) followed by the *tripod* grasp (90.4 ± 3.3%) and *precision disk* (89.4 ± 2.3%). Table 10 presents the average and standard deviation of the activation times of the robotics hand among the correctly classified trials. The average activation time of the robotic hand among all grasp types was 0.54 ± 0.05 s. *Thumb-2 fingers* and *thumb-4 fingers* had the largest variance on the activation time (0.25 s and 0.3 s respectively).

4. Discussion

Previous studies [17,19,26,36], presented different approaches for mapping EMG signals to reaching and grasping motions according to object's features and locations and during static or dynamic gestures. In these approaches, the system is trained as the subject is asked to perform a grasp type, with or without holding an object, and stay there for a few seconds. Using this technique, the classifier is able to recognize different grasp types only after they are already performed. Transferring this method to an on-line application, the hand should, first, travel the distance to object location and then start closing with respect to the preferred grasp type. This equals a mechanical and unnatural motion with respect to the seamless natural motion of the human hand. In the proposed approach, the classifier is trained with data of the reaching motion and the classification performance is related to the time of fingers/hand preshape. A decode of the grasping type in the early stages of the motion is important, as it would enable the device to react promptly to the intention of the user. Therefore,
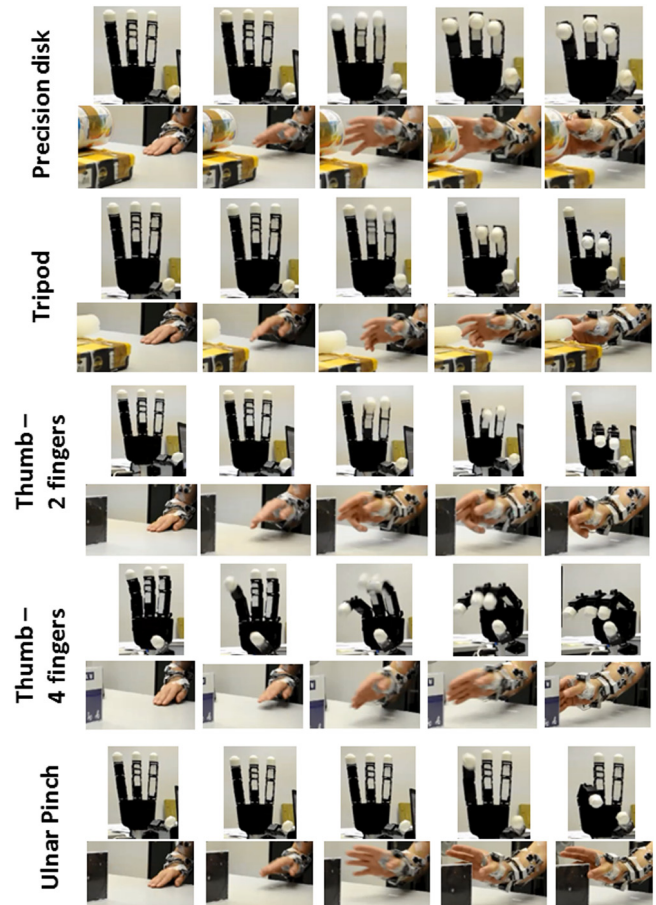

Fig. 10. Snapshots of the finger motions of the robotic hand and human hand.

we here proposed an EMG-based learning approach that decodes the grasping intention of the user at an early stage of the reach to grasp motion. Our approach was based on an Echo State Network (ESN) [34] combined with a Majority Vote (MV) criterion applied to time windows of 150 ms from the motion onset to the grasp of the object. We applied the algorithm to an offline classification of five different grasp types: precision disk, tripod, ulnar pinch, thumb-2 fingers and thumb-4 fingers grasp. Furthermore, we examined whether the proposed approach was robust to different objects' location and to different motion speeds. Indeed, the object's distance and the movement velocity could differentiate the activation of the muscles, especially for the muscles of the upper arm, influencing the classification performance. Finally, we demonstrated in three subjects the usability of our approach for the online control of the Allegro hand.

Reaching-to-grasp motions are decomposed into two phases: (a) the reaching phase, where the hand is traveling toward the object location, and (b) the grasping phase, where the hand has reached the object and the fingers are in contact with the object [21–23]. In natural self-paced motion the hand spontaneously opens and closes while being in the reaching phase [21–23,16]. The preshape of the hand is defined as the formation of the fingers before they take the final configuration, and it takes place during the reaching cycle [33]. More particularly, the fingers extend to a maximum before they start closing (continuously flex) around the object with respect to its characteristics. It has been reported that the posture of the hand could be discriminated well before the contact with the object [24]. In other words, the trajectories of the fingers before their closure around the object correspond to an

indication of the final grasp type before the grasping phase, i.e. before the fingers are in contact with the object. In this paper, we showed that this information could be revealed from the muscular activity.

It was shown that the hand's pre-shaping occurs from 60% to 80% of the reach-to-grasp motion, which corresponds to the time instant when the distance between the thumb and the index reached its maximum [21,33]. Our analysis with normalized time suggested that hand's preshape occurs after the 30% with respect to the completion time of the task. Additionally, we observed that the fingers are preshaping between the 30%–60% of the reaching cycle regardless of the distance from the object or the speed of the motion. Moreover, the initial position of the hand as well as the characteristics of the object could play an important role on the detection of the preshape. More particularly, when reaching to grasp a thin object by starting from an open-hand configuration, the hand may not need to open more in order to adjust to the size of the object. In this case, detecting the preshape becomes less trivial, and additional principles should be considered for the definition of the preshape. At this paper, we considered the onset of a smooth closure of the fingers (flexion without extension) as such a principle. On the other hand, the detection of the preshape becomes more obvious when the task demands large extension of the fingers.

Moreover, it has been suggested that a period between the 25% and the 50% could be sufficient to obtain differences in muscle activity when reaching to grasp three different objects [37]. Expanding this suggestion, our results showed that it is possible to classify five grasp types using EMG data from early stages of the reaching motion. Relating the classification performance with the hand's preshape, our offline results showed that a classification rate of 90% was achieved before the hand preshaping for the precision disk, tripod, and ulnar pinch. For the thumb-2 fingers and the thumb-4 fingers grasps, instead, the computed hand preshape criteria did not always show a peak, thus the hand preshaping was not always clearly detected.

We evaluated the accuracy of our approach by decreasing the number of EMG channels inserted as input to the classifier. By removing the muscles from the hand and forearm, we kept less information regarding the motion of the fingers, expecting that this would influence negatively the performance. The results showed a significant decrease on the classification performance when using 9 and 7 muscles from the initial muscle set. More particularly, the classification performance reduces as one remove the muscles of the hand and forearm, but does not lead to a significant drop in the performance as long as we retained at least 7 muscles from the upper arm and 4 from the forearm (i.e *Flexor Digitorum Superficialis, Flexor Carpi Ulnaris, Extensor Digitorum Communis* and *Extensor Carpi Ulnaris*). These results indicate that our method may successfully classify grasps early without the muscular activity of the more distal muscles. Although the results with less EMG channels are promising, one should keep in mind that the activation of the residual muscles of an amputated arm could be different concluding to a different performance. Keeping that aside, the proposed method performs efficiently with able-bodied users as presented in the online implementation.

In addition, we examined the proposed approach when the object is placed in different distances. Our results showed no significant differences between the classification performance on different object's distances. This outcome may be explained from the training of the classifier in time steps without normalizing the time. With this approach, we were able to capture enough variability of the EMG activity of motions with different duration and speed. Additionally, we took advantage of the short-term memory capacity of the Echo State Networks (ESNs) by avoiding extracting features and treating the signals as time-series. This approach imparted a level of tolerance to different muscle activation to the classifier. Furthermore, we evaluated different combinations of training and testing dataset acquired at different object's distances and we concluded that the best performance was achieved when the classifier was trained in the middle distance and tested in distances 10 cm larger or shorter. Comparing the performances between the same training approaches (as presented in Figs. 5(b) and 5(c)), the lowest classification performances noticed when the classifier was trained with the shorter distance and tested on further distances. This result suggests a better generalization over the shorter distances than the further positions. A potential expansion of the generalization would be the inclusion of different positions in space.

Although no significant differences were found when considering different object's distances, as the motion velocities in self-paced motions may be slightly different depending on the object's location, fast motion influenced significantly the classification performance. Although the preshape appears in the same stage on the reaching cycle regardless the speed of the motion, it is noticed that hand preshapes significantly sooner in time than in self-paced motions. Additionally, in some cases the fingers may follow different trajectories than in self-paced motions. The rapid activation of the arm muscles during fast motions differentiates the activation of agonist/antagonists muscles, influencing the EMG signals and resulting in a lower performance when significantly different velocities were taken into account. A classifier that included different speed motions performed sufficiently well only when the training involved both data form normal and fast motions. The reduction of the performance obtained when the classifier was trained with a single speed motion may cause inconvenient behavior for assistive and prosthetic devices. Therefore, higher attention should be paid to the effect of speed on the design of more human-friendly and convenient robotic devices that should interact with patients. Indeed, comfort and robot–human interfaces represent two pivotal aspects in robotic-rehabilitation approaches.

For a proof of concept, we integrated our approach in the control of an Allegro hand. After a training phase performed offline including 15 repetitions for each object of the five grasp types, the success rate of classification was around 92.5%. The difference between the offline and online classification performance could be due to different sampling frequency used in the online implementation. This robotic implementation leads to the conclusion that the early estimation of the final grasp from the EMG signals could be applied to a robotic system and, as an extension, may be applied to the control of a prosthetic device or of an exoskeleton. An important extension of the approach is the introduction of a robotic control scheme that derives from the natural motion of the human hand, which would impart a human-like behavior to the robotic device. Additional works could be done to integrate to the robotic system tactile sensors for the attainment of a safe/stable grasp. Indeed, recent developments on the sensory field [38,39], showed that the design of compliant prosthesis should also include the sensory feedback to the user. This feedback could involve visual and tactile information in order to provide a compliant solution to the demands of the different conditions. A control scheme of an upper arm prosthesis that combines a variety of sensors (e.g EMG, vision, tactile sensors) would provide a robust use of the device . Moreover, a potential next step would be to include the proposed approach into the control of a fingers' exoskeleton in order to examine any inconvenience that this may cause and be further developed on a semi-autonomous control scheme.

Moreover, it has been reported [27] that it possible to relate the object's characteristics with the muscular activity. Toward this direction, the decode of the preshape by the EMG signals, as presented in our work, could provide valuable information for object before the contact of the fingers with the object. As this

information comes in advance of the contact, it could be potentially used for accomplishment of a safe grasp.

Finally, a further interesting extension of this work is the classification of specific finger configuration with different hand orientations. In this case, a classifier could tackle the problem of the high dimensionality of the task with the use of postural synergies [16], which correspond to a number of hand postures that humans combine when grasping. Furthermore, during grasping different orientations of the hand are used. Studies [40,41,42] has reported a successful classification of the simultaneous motion of the wrist and fingers. A potential combination of the decode of the grasping intention of the user with the simultaneous control of the wrist will provide a more natural motion of the wearable device with respect to the human motion.

5. Conclusion

In this paper we propose an electromyographic based approach for decoding the grasping intention in reach-to-grasp motions. Our results have shown that it is possible to decode the grasping intention in the early stages of the reaching motion during the hand's preshape, i.e. before the fingers final configuration. This is very important for proper reaction of the wearable device and the increase of the natural motion of a prosthesis. Further extensions should involve the evaluation of the proposed approach in different hand's orientation and different object's positions in space.

Acknowledgments

References

[1] O. Lambercy, L. Dovat, H. Yun, S.K. Wee, C.W.K. Kuah, K.S.G. Chua, R. Gassert, T.E. Milner, C.L. Teo, E. Burdet, Effects of a robot-assisted training of grasp and pronation/supination in chronic stroke: a pilot study, J. Neuroeng. Rehabil. 8 (63) (2011).

[2] E. Biddiss, Need-directed design of prostheses and enabling resources in: Amputation, Prosthesis Use, and Phantom Limb Pain: An Interdisciplinary Perspective, 2010.

[3] P. Maciejasz, J. Eschweiler, K. Gerlach-Hahn, A. Jansen-Troy, S. Leonhardt, A survey on robotic devices for upper limb rehabilitation, J. Neuroeng. Rehabil. 11 (3) (2014).

[4] D. Novak, R. Riener, A survey of sensor fusion methods in wearable robotics, Robot. Auton. Syst. (2014).

[5] Z.O. Khokhar, Z.G. Xiao, C. Menon, Surface EMG pattern recognition for real-time control of a wrist exoskeleton, Biomed. Eng. Online 9 (2010) 41–57.

[6] A. Ziai, C. Menon, Comparison of regression models for estimation of isometric wrist joint torques using surface electromyography, J. Neuroeng. Rehabil. 8 (2011) 56–67.

[7] D. Nishikawa, W. Yu, H. Yokoi, Y. Kakazu, EMG prosthetic hand controller using real-time learning method, in: Proceedings of the IEEE International Conference on Systems, Man, and Cybernetics, SMC, 1999.

[8] Z. Ju, H. Liu, Human Hand Motion Analysis With Multisensory Information, IEEE/ASME Trans. Mechatronics 19 (2) (2014).

[9] O. Fukuda, T. Tsuji, M. Kaneko, A. Otsuka, A human-assisting manipulator teleoperated by EMG signals and arm motions, IEEE Trans. Robot. Autom. 19 (2) (2003).

[10] F. Sebelius, M. Axelsson, N. Danielsen, J. Schouenborg, T. Laurell, Real-time control of a virtual hand, Technol. Disabil. 17 (2005) 131–141.

[11] P. Shenoy, K.J. Miller, B. Crawford, R.P.N. Rao, Online electromyographic control of a robotic prosthesis, IEEE Trans. Biomed. Eng. 55 (3) (2008).

[12] Y. Huang, K.B. Englehart, B. Hudgins, A.D.C. Chan, A Gaussian mixture model based classification scheme for myoelectric control of powered upper limb prostheses, IEEE Trans. Biomed. Eng. 52 (11) (2005).

[13] K. Kita, R. Kato, H. Yokoi, Tamio Arai, Development of autonomous assistive devices-analysis of change of human motion patterns, in: IEEE International Symposium on Robot and Human Interactive Communication, RO-MAN, 2006.

[14] M.W. Jiang, R.C. Wang, J.Z. Wang, D.W. Jin, A method of recognizing finger motion using wavelet transform of surface EMG signal, in: Proceedings of the IEEE Engineering in Medicine and Biology 27th Annual Conference, 2005.

[15] L.A. Jones, S.J. Lederman, Human Hand Function, Oxford University Press, 2006.

[16] M. Santello, M. Flanders, J.F. Soechting, Postural hand synergies for tool use, J. Neurosci. (1998).

[17] S.A. Dalley, H.A. Varol, M. Goldfarb, A method for the control of multigrasp myoelectric prosthetic hands, IEEE Trans. Neural Syst. Rehabil. Eng. 20 (1) (2012).

[18] C. Sapsanis, G. Georgoulas, A. Tzes, D. Lymberopoulos, Improving EMG based classification of basic hand movements using EMD, in: Proceedings of the IEEE Engineering in Medicine and Biology 35th Annual Conference, 2013.

[19] G. Ouyang, X. Zhu, Z. Ju, H. Liu, Dynamical characteristics of surface EMG signals of hand grasps via recurrence plot, IEEE J. Biomed. Health Inform. 18 (1) (2014).

[20] R.J. Smith, F. Tenore, D. Huberdeau, R. Etienne-Cummings, N.V. Thakor, Continuous decoding of finger position from surface EMG signals for the control of powered prostheses, in: Proceedings of the IEEE Engineering in Medicine and Biology 30th Annual Conference, 2008.

[21] Y. Paulignan, C. MacKenzie, R. Marteniuk, M. Jeannerod, The coupling of arm and finger movements during prehension, Exp. Brain. Res. 79 (1990) 431–435.

[22] M. Jeannerod, The timing of natural prehension movements, J. Motor Behav. 16 (3) (1984).

[23] M. Jeannerod, Y. Paulignan, P. Weiss, Grasping an object: one movement, several components, in: Novartis Foundation Symposium, 1998.

[24] M. Santello, J.F. Soechting, Gradual molding of the hand to object contours, J. Neurophysiol. 79 (3) (1998).

[25] J. González, Y. Horiuchi, W. Yu, Classification of upper limb motions from around-shoulder muscle activities: Hand biofeedback, Open Med. Inform. J. (2010).

[26] M.V. Liarokapis, P.K. Artemiadis, K.J. Kyriakopoulos, E.S. Manolakos, A learning scheme for reach to grasp movements: On EMG-based interfaces using task specific motion decoding models, IEEE J. Biomed. Health Inform. 17 (5) (2013).

[27] N. Fligge, H. Urbanek, P. van der Smagt, Relation between object properties and EMG during reaching to grasp, J. Electromyogr. Kinesiol. 23 (2013) 402–410.

[28] I.M. Bullock, J.Z. Zheng, S. De La rosa, C. Guertler, A.M. Dollar, Grasp frequency and usage in daily household and machine shop tasks, IEEE Trans. Haptics 6 (3) (2013).

[29] R.C. Oldfield, The assessment and analysis of handedness: The Edinburgh inventory, Neuropsychologia 9 (1971) 97–113.

[30] H.J. Hermens, et al., Development of recommendations for SEMG sensors and sensor placement procedures, J. Electromyogr. Kinesiol. 10 (5) (2000) 361–374.

[31] R.L. de Souza, R.L. S. El-Khoury, J. Santos-Victor, A. Billard, Towards comprehensive capture of human grasping and manipulation skills, in: Proceedings of the Thirteenth International Symposium on the 3-D Analysis of Human Movement, 2014.

[32] P. Haggard, A. Wing, Coordinated responses following mechanical perturbation of the arm during prehension, Exp. Brain. Res. 102 (1995) 483–494.

[33] T. Supuk, T. Kodek, T. Bajd, Estimation of hand preshaping during human grasping, Med. Eng. Phys. 29 (2005) 790–797.

[34] H. Jaeger, The "echo state" approach to analyzing and training recurrent neural networks, GMD Report 148, GMD - German National Research Institute for Computer Science, 2001.

[35] K. Englehart, B. Hudgins, a Robust and real-time control scheme for multifunction myoelectric control, IEEE Trans. Biomed. Eng. 50 (7) (2003).

[36] J. Carpaneto, K.H. Somerlik, T.B. Krueger, T. Stieglitz, S. Micera, Natural muscular recruitment during reaching tasks to control hand prostheses, in: IEEE RAS & EMBS International Conference on Biomedical Robotics and Biomechatronics, 2012.

[37] S. Martelloni, J. Carpaneto, S. Micera, Characterization of EMG patterns from proximal arm muscles during object- and orientation-specific grasps, IEEE Trans. Biomed. Eng. 56 (2009) 2529–2536.

[38] S. Raspopovic, M. Capogrosso, F.M. Petrini, M. Bonizzato, J. Rigosa, G. Di Pino, J. Carpaneto, M. Controzzi, T. Boretius, E. Fernandez, G. Granata, C.M. Oddo, L. Citi, A.L. Ciancio, C. Cipriani, M.C. Carrozza, W. Jensen, E. Guglielmelli, T. Stieglitz, P.M. Rossini, S. Micera, Restoring natural sensory feedback in real-time bidirectional hand prostheses, Sci. Transl. Med. 6 (222) (2014).

[39] D. Novak, X. Omlin, R. Leins-Hess, R. Riener, Effectiveness of different sensing modalities in predicting targets of reaching movements, in: International Conference of the IEEE EMBS, 2013.

[40] A.J. Young, L.H. Smith, E.J. Rouse, L.J. Hangrove, Classification of simultaneous movements using surface EMG pattern recognition, IEEE Trans. Biomed. Eng. 60 (5) (2013).

[41] A. Fougner, O. yvind Stavdahl, P.J. Kyberd, System training and assessment in simultaneous proportional myoelectric prosthesis control, J. Neuroeng. Rehabil. 11 (2014) 75.

[42] F.P. Kendall, E. Kendall McCreary, P. Geise Provance, M. McIntyre Rodgers, W.A. Romani, Muscles Testing and Function with Posture and Pain, fifth ed., Lippincott Williams & Wilkins, 2005.

Iason Batzianoulis received his Diploma in Electrical and Computer Engineering from Aristotle University of Thessaloniki, Greece, in 2012. He is currently working toward the Ph.D. degree with Learning Algorithms and Systems Laboratory, Swiss Federal Institute of Technology in Lausanne (EPFL), Lausanne, Switzerland.

His research interest include human-oriented methods for controlling robotic hands. He is also interested in the development of control algorithms for wearable devices.

Sahar El-Khoury is a postdoctoral fellow at EPFL (Switzerland). She has an Electrical Engineering Degree from Ecole Superieure d' Ingenieurs de Beyrouth in 2004. She received her M.Sc. and Ph.D. degree in Robotics and Intelligent Systems from Universite Pierre et Marie Curie (Paris 6) in 2005 and 2008. Her research interests have been focused on grasp planning and manipulation.

Elvira Pirondini received the B.S. in biomedical engineering from the Politenico of Milan in 2010 and the M.S. degree in bioengineering from the Swiss Federal Institute of Technology in Lausanne (EPFL), Lausanne, Switzerland in 2012. She is currently a Ph.D. student in the Translational Neural Engineering Laboratory at the EPFL.

Her research interests concern the study of brain plasticity following a stroke and during the recovery process applying new signal processing techniques based on the combination of electroencephalography and electromyography activity.

Martina Coscia received the Master degree in Biomedical Engineering from the University of Pisa, Pisa, Italy, in 2009, and the Ph.D. degree in Biorobotics from the Scuola Superiore Sant' Anna, Pisa, Italy, in 2013. From 2013, she is a Post-doctoral Fellow at the Swiss Federal Institute of Technology in Lausanne (EPFL), Lausanne, Switzerland. In 2011–2012, she was a visiting student of the Motion Analysis Lab at the Spaulding Rehabilitation Hospital, Boston, Massachusetts, USA.

Her research is about neurorehabilitation of stroke subjects. In particular, she is interested in the study of the motor control of post-stroke subjects in order to design innovative strategies for neurorehabilitation.

Silvestro Micera (S'94–M'99–SM'06) received the University degree (Laurea) in electrical engineering from the University of Pisa, Pisa, Italy, in 1996, and the Ph.D. degree in biomedical engineering from the Scuola Superiore Sant' Anna, Italy, in 2000.

From 2000 to 2009, he has been an Assistant Professor of BioRobotics at the Scuola Superiore SantAnna, where he is now Associate Professor and the Head of the Neural Engineering group. In 2007, he was a Visiting Scientist at the Massachusetts Institute of Technology, Cambridge, USA with a Fulbright Scholarship. From 2008 to 2011, he was the Head of the Neuroprosthesis Control group and an Adjunct Assistant Professor at the Institute for Automation, Swiss Federal Institute of Technology, Zurich, CH. Since 2011, he has been Associate Professor and Head of the Translational Neural Engineering Laboratory at the EPFL. His research interests include the development of hybrid neuroprosthetic systems (interfacing the central and peripheral nervous systems with artificial systems) and of mechatronic and robotic systems for function and assessment restoration in disabled and elderly persons. He is the author of more than 80 ISI scientific papers and several international patents.

Dr. Micera received the "Early Career Achievement Award" of the IEEE Engineering in Medicine and Biology Society in 2009. He is currently an Associate Editor of the IEEE TRANSACTIONS ON BIOMEDICAL ENGINEERING AND THE IEEE TRANSACTIONS ON NEURAL SYSTEMS AND REHABILITATION ENGINEERING. He is also Member of the Editorial Boards of the Journal of Neuroengineering and Rehabilitation and of the Journal of Neural Engineering.

Aude Billard received the M.Sc. degree in physics from the Swiss Federal Institute of Technology in Lausanne (EPFL), Lausanne, Switzerland, in 1995, and the M.Sc. degree in knowledge-based systems and the Ph.D. degree in artificial intelligence from the University of Edinburgh, Edinburgh, UK, in 1996 and 1998, respectively.

She is currently a Professor of micro and mechanical Engineering and the Head of the Learning Algorithms and Systems Laboratory, School of Engineering, EPFL. Her research interests include machine learning tools to support robot learning through human guidance. This also extends to research on complementary topics, including machine vision and its use in human–robot interaction and computational neuroscience to develop models of motor learning in humans.

Dr. Billard received the Intel Corporation Teaching Award, the Swiss National Science Foundation Career Award in 2002, the Outstanding Young Person in Science and Innovation from the Swiss Chamber of Commerce, and the IEEE-RAS Best Reviewer Award in 2012. She served as an Elected Member of the Administrative Committee of the IEEE Robotics and Automation Society (RAS) for two terms (2006–2008 and 2009–2011) and is the Chair of the IEEE-RAS Technical Committee on Humanoid Robotics.